Published in final edited form as:
Expert Opin Med Diagn. 2011 May 1; 5(3): 241–251.

Exogenous near-infrared fluorophores and their applications in cancer diagnosis: biological and clinical perspectives

Hua Zhang, Ph.D[Assistant Professor], **Ryan R. Uselman**, and **Douglas Yee**
Department of Medicine, Masonic Cancer Center, MMC 806, 420 Delaware St SE, Minneapolis, MN, 55455, USA, Phone: 612-626-2838, Fax: 612-624-3913

Hua Zhang: zhang334@umn.edu

Abstract

Introduction—Near-infrared fluorescent (NIRF) imaging is a rapidly growing research field which has the potential to be an important imaging modality in cancer diagnosis. Various exogenous NIR fluorophores have been developed for the technique, including small molecule fluorophores and nanoparticles. NIRF imaging has been used in animal models for the detection of cancer overthe last twenty years and has in recent years been used in human clinical trials.

Areas covered—This article describes the types and characteristics of exogenous fluorophores available for in vivo fluorescent cancer imaging. The article also discusses the progression of NIRF cancer imaging over recent years and its future challenges, from both a biological and clinical perspective. in The review also looks at its application for lymph node mapping, tumor targeting and characterization, and tumor margin definition for surgical guidance.

Expert Opinion—NIRF imaging is not in routine clinical cancer practice; yet, the authors predict that techniques using NIR fluorophores for tumor margin definition and lymph node mapping will enter clinical practice in the near future. The authors also anticipate that NIRF imaging research will lead to the development of flurophores with ‘high brightness’ that will overcome the limited penetration of this modality and be better suited for non invasive tumor targeting

1. Introduction

Various imaging modalities exist to facilitate cancer diagnosis and staging, determine the efficacy of cancer treatment, and detect recurrence. Among these, X-rays, computer assisted tomography (CAT) scanning, magnetic resonance imaging (MRI), and ultrasonography provide important information regarding tumor size and location. Methods of radionuclide imaging, such as positron emission tomography (PET) and single photon emission computed tomography (SPECT), have the additional capacity to measure tumor metabolism, and in some cases, detect the levels of cell surface markers within a tumor [1–3].

In addition to these imaging modalities, fluorescent imaging has emerged with unique capabilities for molecular cancer imaging. Fluorescence is the light emitted by certain molecules when they absorb light at a shorter wavelength (excitation). These fluorophores emit energy throughout the visible spectrum; however, the best spectrum for *in vivo* imaging is in the near-infrared (NIR) region (650 nm-900 nm) [4]. Unlike the visible light spectrum

Correspondence to: Hua Zhang, zhang334@umn.edu.

Declaration of Interest
This work is supported by a grant given by the National Institutes of Health (R01CA74285) to D Yee in addition to a National Cancer Institute Cancer Centre Support Grant P30 077598.

(400–650 nm), in the NIR region, light scattering decreases and photo absorption by hemoglobin and water diminishes, leading to deeper tissue penetration of light. Furthermore, tissue auto-fluorescence is low in the NIR spectra, which allows for a high signal to noise ratio [4].

In this review, we describe the types and characteristics of exogenous fluorophores available for *in vivo* NIR fluorescent (NIRF) cancer imaging. We also address recent progress and future challenges of cancer imaging applications, such as lymph node mapping, tumor targeting and characterization, and surgical guidance, from biological and clinical perspectives. The instruments and methodology of whole body fluorescent imaging are not within the scope of this review and have been reviewed elsewhere [5].

2. Types of NIR fluorescent (NIRF) imaging probes

2.1. Small molecule organic fluorophores

There is a range of small molecule organic fluorophores with excitation and emission spectra in the NIR region. Some, such as indocyanine green (ICG) and cyanine derivatives Cy5.5 and Cy7, have been used in imaging for a relatively long time. Modern fluorophores are developed by various biotechnology companies and include: Alexa dyes [6]; IRDye dyes; VivoTag dyes and HylitePlus dyes. In general, the molecular weights of these fluorophores are below 1 kDa. Some of these newly developed dyes have relatively high brightness due to their high extinction coefficients, and have better characteristics, such as resistance to photobleaching and less non-specific binding. The Alexa dyes are more resistant to photobleaching than the Cy5.5 and Cy7 dyes [7]. In addition, Ogawa *et al.* compared Alexa 680 and Cy5.5 conjugates and found that Cy5.5 conjugates produced nonspecific results and rapid liver accumulation; in contrast, Alexa 680 conjugates demonstrated specific targeting with low background [8]. Most small molecule fluorophores are water-soluble and carry reactive groups that allow conjugation with antibodies, peptides, or nucleic acids. By controlling the ratio and reaction time, these dyes have been optimized to link one or two biomolecules. Because of their small molecular weights, when the fluorophores are chemically linked to larger molecular weight biomolecules, such as antibodies, the pharmacokinetics of the conjugates tend to be similar to those of the biomolecules and not the organic fluorophores [9–11].

2.2. Quantum dots

Quantum dots (QDs) are semiconductor nanoparticles that emit fluorescence upon excitation with a light source. Depending on their chemical composition, QDs can emit fluorescence throughout the visible spectrum and into the NIR region. The majority of QDs are binary semiconductor crystals composed of two types of atoms from the II/VI [12,13] or III/V [14] group elements on the periodic table. In general, each QD is composed of a binary crystal core and capped with a binary shell that stabilizes and increases its quantum yield (Figure 1). The surfaces of these nanocrystals are passivated with a monolayer of organic solvent, such as tri-n-octylphosphine oxide (TOPO) [15]. TOPO passivated QDs are hydrophobic and insoluble in aqueous solutions. To achieve water solubility and biocompatibility, QDs are often encapsulated with various types of amphiphilic polymers, which increase their hydrodynamic radius to about 10–20 nm. These amphiphilic polymers often carry chemically reactive groups, such as amines and carboxylic acids that allow conjugation with biomolecules such as peptides, proteins, and nucleic acids. Encapsulation and bioconjugation do not usually alter the optical properties of QDs significantly [16].

Although Cadmium selenide (Cd/Se) QDs are the best studied, they are not very suitable for *in vivo* imaging due to their short emission wavelength (470–655 nm). The so-called type II QDs emit fluorescence in the far-red and NIR range, which makes them ideal for *in vivo*

cancer imaging. A type II QD consists of a Cd/Te core with a Cd/Se (or ZnS) shell; the increased thickness of their shell correlates with their higher emission wavelength [17,18].

For imaging purposes, QDs have several advantages over small molecule organic fluorophores. QDs have higher brightness due to their high quantum yield and high molar-extinction coefficients. At their optimal excitation spectra, the extinction coefficients of QDs can reach 10^6–10^7 M^{-1} cm, about 10 to 100 times larger than those for most organic dyes. QDs also possess high photo-bleaching thresholds, as well as broad excitation spectra and narrow, symmetric emission spectra. This last property of QDs allows simultaneous detection of multiple fluorescent signals using a single excitation light source.

However, QDs also have a few disadvantages over small molecule fluorophores. Small molecule fluorophores have narrow “Stokes shift”, meaning that their optimal excitation and emission spectra are fairly close (normally within 50 nm). Therefore, NIRF can be performed using their optimal excitation and emission wavelength. In contrast, the optimal excitation wavelength of QDs, including the type II QDs, is shorter than 400 nm. To avoid tissue absorbance and light scattering, the excitation wavelength for *in vivo* QD imaging is often compromised to the near NIR region [19,20], at which QDs’ extinction coefficients drop significantly [21]. Another disadvantage of QDs is their large size. The pharmacokinetics of conjugates tends to be similar to QDs, instead of the conjugated biomolecules. Therefore, QD conjugates may fail to serve as a tracer to track the circulation of biomolecules *in vivo*.

2.3. Fluorophore-doped nanoparticles

Doping, a term often used in the semiconductor field, refers to intentionally introducing impurities into a semiconductor to change its properties. Recently, a few research groups have developed fluorophore-doped nanoparticles encapsulated by amphiphilic polymers [22,23]. These nanoparticles tend to have high brightness due to the large number of encapsulated fluorophores and high photostability due to their polymer coating, which prevents penetration of oxygen and reduces bleaching [24]. Compared with the other two types of fluorophores, the flurophore-doped nanoparticles have not been well studied in their characteristics and *in vivo* imaging capabilities.

3. *In vivo* imaging applications in cancer

The complexity of mammalian anatomy and physiology poses several challenges for *in vivo* fluorescent imaging not present *in vitro*. First of all, imaging probes must be photostable to allow for real-time and long term imaging. Second, conjugated imaging probes must be chemically stable and avoid degradation in the circulation in order to reach target cancer cells. Third, safety concerns demand non-toxic conjugated imaging probes that are quickly cleared, either by excretion through the urinary system or gradual degradation in the liver. Finally, non-invasive imaging in deep tissue requires probes with strong emission fluorescence. Over the past twenty years, many NIRF imaging agents have been developed and intensively studied in cancer imaging, particularly lymph node mapping, tumor target and characterization, and surgical guidance. These techniques are discussed herein from biological and clinical perspectives.

3.1. Lymph node mapping

Metastasis is the leading cause of cancer death and begins when cancer cells move from the primary site of origin to nearby lymph nodes. Frequently, a sentinel lymph node (SLN) is the first lymph node or group of nodes to receive metastasized cells. SLN biopsy identifies and removes SLNs to determine whether the primary tumor has metastasized. This procedure is routinely used in the clinic to assess the stage and prognosis of breast cancer

and melanoma [25]. Current mapping techniques include peritumoral injection of radioisotopes, isosulfan blue dyes, or a combination of both agents.

Type II QDs, have been extensively studied in SLN mapping experiments [18,26–29]. In the pioneer study by Kim *et al.*, mice and pigs were intradermally injected with Type II QDs coated in polydentate phosphine, which renders QDs soluble and stable, and they rapidly drained into the nearest SLN [18]. Because QDs have very high brightness, they were visible through the tissue, even before a surgical incision was made. The high brightness of QDs presents a major advantage over blue dye; however, extra equipment would be required to excite the QDs and collect their emission spectra.

Organic fluorophores, mainly ICG, have also been utilized in SLN mapping. ICG, a small molecule fluorophore with a molecular weight of 775 Da, has been approved by the Food and Drug Administration (FDA) as a contrast agent for measuring tissue blood volume, cardiac output, ophthalmic angiography and hepatic function [30–32]. ICG has a very high safety profile for human use, and several studies have assessed its potential for SLN mapping in human clinical trials [33–36]. These results were very promising, and the use of fluorescent dyes could have advantages over the use of raidioisotopes, such as the lack of both ionic radiation and the need for appropriate logistics for radioactive matter.

In many other types of cancer, SLN biopsy is a well accepted concept, but several challenges prevent its clinical application. Visceral organs, such as the gastrointestinal tract, lungs, and prostate gland, have complex lymphatic drainage systems that make SLN mapping very challenging [27,37]. Furthermore, the lymph nodes of the thoracic esophagus can be pigmented, which makes it difficult to visualize isosulfan blue dye [37]. Multiple fluorophores of different emission wavelengths could be used to identify and sort these complicated lymphatic systems. Work from Kobayashi's group has demonstrated the feasibility of mapping multiple lymph nodes using various small molecule fluorophores in combination with QDs [19,21,38,39]. In one of their studies, five QDs with different emission wavelengths were intracutaneously injected at five different sites in the mice: the middle phalanges of the left or right upper extremity, the left and right ear, and the median chin; all of which contain complicated lymphatic networks. After injection, the lymphatic drainages of the neck and upper trunk were closely monitored using real time *in vivo* imaging. In total, five different lymphatic basins were successfully mapped and validated by *ex vivo* fluorescence imaging of dissected lymph nodes [21].

3.2. Tumor targeting and characterization

Certain molecules are often solely expressed or overexpressed in specific types of cancer. For instance, MUC1 (CD227) is overexpressed in 90% of human breast cancers [40], and prostate-specific membrane antigen (PSMA) is highly expressed on the surface of prostate tumors [41]. In addition, some proteins, such as folate receptor [42] and transferrin receptor [43] are highly expressed on the surface of certain types of tumors. These highly expressed proteins or molecules can serve as molecular targets for fluorescent imaging probes and help locate tumors and metastatic lesions. Various proof of principle experiments have been performed in primary tumor sites to validate this concept [15,44,45]. In a recent study, a small molecule that binds PSMA was conjugated with ICG, and these conjugates specifically identified PSMA in xenograft mouse tumors [46]. Similarly, Gao *et al.* have demonstrated that PSMA conjugated QDs injected intravenously into mice will localize to xenograft prostate tumors [15].

In addition to tumor antigens, various transmembrane receptor tyrosine kinases are often overexpressed in cancer. For instance, human epidermal growth factor receptor-2 (HER2) is overexpressed in about 20–30% of breast cancer [47]. These receptor tyrosine kinases play

important roles in cancer cell proliferation, motility, and metastasis, which make them ideal molecular targets for cancer therapy. Targeted therapies against these receptors have been aggressively pursued over the past twenty years and have proven their clinical benefit. However, selecting patients that will respond to these targeted therapies remains a significant challenge.

Since receptor expression is necessary, imaging techniques that detect and quantify receptor levels have practical application in the selection process. Numerous *in vivo* imaging studies have been performed to localize and measure receptor levels in mouse tumor models, particularly levels of HER2 [47,48] and epidermal growth factor receptor (EGFR). For example, Ke *et al.* have shown that EGF conjugated Cy5.5 specifically targeted mouse xenograft tumors expressing EGFR, but did not bind to mouse xenograft tumors lacking EGFR [9]. Similarly, work from Zhang *et al.* have shown that an Alexa 680 conjugated antibody against type I IGF receptor (IGF1R) targeted tumors expressing IGF1R and was able to detect downregulation of IGF1R in mouse xenograft tumors [20]. Furthermore, two or more fluorescent conjugates have been used to distinguish the expression pattern of various receptor tyrosine kinases on the cell surface [49,50]. In Barrett *et al.*'s study, Cy5.5-labeled cetuximab (anti-EGFR) and Cy7-labeled trastuzumab (anti-HER2) were intravenously injected into mice bearing xenograft tumors overexpressing either EGFR or HER2. Subsequent multiplex imaging on Cy5.5 and Cy7 clearly differentiated the two tumor types in the mice [50].

In contrast to lymph node mapping, tumor targeting and characterization are much more challenging. Tumor targeting fluorophores must be conjugated to antibodies or peptides for specific molecular interactions to take place on the cancer cell surface. Depending on the specificity of these molecular interactions, the pharmacokinetics of the fluorophore conjugates, and the expression levels of the targeted molecules on the tumor and surrounding tissue, high background can limit imaging sensitivity. To solve this problem, so called "activatable probes" have been developed. The fluorescence of these NIRF probes is quenched initially, then "activated" after they bind tumor cells. Weissleder and his colleagues have developed activatable probes that are recognized by proteinases such as cathepsin D and matrix metalloproteinases (MMP)-2 [51–53]. In one of their designs, a poly-L-lysine backbone contains multiple MMP cleavage sequences and carries Cy5.5 at the end of the construct. The addition of methoxy polyethylene glycol *(MPEG)* side chains to the construct allows for improved pharmacokinetics (Figure 2). Due to the proximity of the fluorochromes, fluorescence resonance energy transfer prevented almost any detectable fluorescent signal in the nonactivated state. When the conjugates reached tumors that expressed MMP-2, the MMP-2 peptide-cleaved spacer and Cy5.5 were released from the carrier, and Cy5.5 became brightly fluorescent. In addition, Tsien's group has developed various activatable cell penetrating peptides (ACPPs) [54–57]. These ACPPs consist of a fluorophore tagged cationic peptide chemically attached to a short stretch of acidic residues via a cleavable linker (Figure 3). The acidic residues prevent cellular uptake of the cationic peptide, but the cleavable linker can be engineered to contain a MMP recognition site. When ACPPs reached tumor surfaces expressing MMPs, the linker on ACPPs was cleaved, releasing the acidic inhibitory domain, and the cationic peptides were free to carry the fluorophore into cells. Due to their unique properties, activatable probes have been sought after by many research groups. Weissleder's activatable probes recently became commercially available and have been applied to various cancer imaging studies [58–60].

Using MMPs to "activate" fluorescent probes allows tumor specificity. However, MMPs are also significantly up-regulated in general inflammatory processes, which may limit their tumor specificity [61]. Recent works by Ogawa *et al.* have shown that targeted self-quenching probes and targeted fluorophore-quencher based activatable optical probes not

only exhibit high tumor specificity and excellent signal to background ratios, but also have the ability to characterize receptor levels on the tumor surface [8,62–64]. Ogawa *et al.* described a self-quenching probe where Alexa 680 was conjugated to trastuzumab (anti-HER2 antibody). The antibody-fluorophore conjugates were non-fluorescent in circulation and only became fluorescent when internalized into the targeted tumor. This occurred after Alexa 680 was cleaved from the conjugates in the lysosomes of tumor cells [8]. Targeted fluorophore-quencher based activatable probes do not have fluorescence outside the cancer cells due to the fluorophore quencher interaction based on fluorescence resonance energy transfer (FRET) quenching [62]. Fluoroscence was detected when the conjugates were internalized into cancer cells and dissociated in lysosomes. These types of activatable probes not only can serve to specifically localize and characterize tumors and metastases, but also have therapeutic potential, depending on the targeting antibody utilized.

While reagents for lymph node mapping can be administered through local injection and subsequently drain into the nearby lymph nodes, tumor-homing conjugates must be administrated intravenously and need to extravasate to reach tumor cells. Due to their small size, organic fluorophore conjugates readily extravasate from the blood stream. However, the large size of QDs and organic-fluorophore doped nanoparticles may limit their ability to extravasate and reach tumor sites. The literature regarding this issue is inconsistent. In the work by Cai *et al.*, RGD (Arg-Gly-Asp) peptide-conjugated QDs that recognize $\alpha_v\beta_3$ integrin were intravenously delivered to mice carrying U87MG human glioblastoma tumors. QD fluorescence was observed in the tumor as quickly as twenty minutes after injection and reached maximum intensity six hours after injection. Interestingly, confocal microscopic analysis of the harvested tumor tissue revealed that the QD fluorescence was retained in tumor vasculature, not within tumor cells. Similar results were also reported in several other studies using QDs delivered intravenously [65–68]. In contrast, other reports have shown QDs extravasated and reached tumors, although the percentage of QD population that reached the tumors was not reported [69,70]. The inconsistent results in the literature reflect the limited amount of research into the characteristics of QDs. Factors that influence QD biodistribution, such as size, surface chemistry, and surface charge, need to be further investigated and clarified [71].

3.3. Surgical guidance: define tumor margin

Surgical removal of most types of cancer, such as breast, head and neck, brain, and melanoma, requires differentiation between the tumor margin and the surrounding normal tissue. Failure to completely remove tumor tissue often results in local recurrence after surgical excision, while removal of healthy tissue (wide margins) along with tumor tissue can disrupt normal organ function and/or have cosmetic impacts. It is therefore crucial to develop imaging techniques that clearly define tumor margins. This type of research greatly corresponds with tumor targeting research; yet, specific differences exist between these two fields of study. In general, tumor targeting requires specific interactions between fluorophore conjugates and molecules on the tumor surface, whereas tumor margins can be defined in two ways. The simplest way is to inject non-conjugated fluorophores systematically after the tumor location has been detected by another imaging modality, such as CAT scanning. Since tumors often have leaky vasculature and lack efficient lymphatic drainage systems, fluorophores may be preferentially retained in the tumor, creating a clear tumor margin against surrounding tissue. Organic fluorophores, mainly indocyanine green (ICG), have been utilized to define tumor margin [72,73]. In Gotoh *et al.*'s clinical trial study, ten patients with hepatocellular carcinoma were systematically injected with ICG a few days before the surgery. During surgery, all ten tumors showed clear margins against surrounding tissue, and were completely removed with negative pathologic margins under the guide of NIRF imaging [73].

Alternatively, tumor margins can be defined through specific interactions between fluorophore conjugates and molecules on the tumor surface. Like tumor targeting and characterization, this technique is still in the early stages of development. However, protease activatable fluorophores are commercially available and have been used to define tumor margins for surgical procedures in mouse orthotropic models [58–60]. In Seth *et al.'s* study, mice were injected intraperitoneally with OVCAR-3 (a human metastatic ovarian cancer cell line) to form metastatic foci in the peritoneal cavity. After the foci formed, ProSense 750 (VisEn Medical), a protease activatable probe, was injected into the tail vein of the mice. One day later, NIRF imaging was performed to guide the surgical removal of the metastatic foci. Based on fifty-two histologically validated samples, the sensitivity for NIRF imaging was 100% accurate in detecting metastatic foci [59]. In addition, ACPPs developed by Tsien's group were used to localize tumors and define tumor margins during surgical removal. Cy5-labeled ACPPs were intravenously delivered to mice and resulted in clearly defined tumor margins against adjacent tissue. ACPP guided tumor resection was more precise than non-imaging guided surgery, and mice whose tumors were resected with ACPP guidance had better long-term tumor-free survival and overall survival than animals whose tumors were resected with traditional bright-field illumination [74].

4. Challenges

4.1. Toxicity

In order for bio-reagents to be used in human clinical applications, they must be non-toxic and have quick clearance, either through biodegradation (metabolism) in the liver or excretion in urine. Because QDs are made of heavy metals, toxicity has been a major concern since their inception. Choi *et al.* have studied renal clearance of QDs in mice [75] and found that QDs with a hydrodynamic diameter below 5.5 nm could be excreted in urine, whereas QDs with a hydrodynamic diameter above 15 nm could not be cleared through the urinary system. Unfortunately, most type II QDs for NIRF imaging have a hydrodynamic diameter above 15 nm [21]. It is noteworthy that no acute toxicity has been observed in mouse studies [68,76–78] because the QD's heavy metal cores are "buried" beneath a polymer coating. However, if these QDs were not eliminated from the mice's bodies and were retained in tumor and non-specific uptake sites, their biodegradable polymer coating might wear away and expose their non-degradable heavy metal core, resulting in toxicity. The short life span of mice compared with human prevents long term studies of the toxicity issue. In this regard, QDs made of non-toxic materials, such as silicon [79–81], may be better suited for future studies. The emission spectra of silicon QDs are also controllable based on the reaction time and synthesis methodology, and can range from blue to the NIR region [82]. However, the methodology to solubilize silicon QDs in aqueous solution has not been well studied and further efforts are needed to move this research area forward.

Choyke and his colleagues searched twenty six comprehensive biomedical and chemical literature databases and conducted a thorough literature review on the toxicity of nineteen widely used organic fluorophores, including four NIR fluorophores [83]. The toxicity of the most commonly used fluorophore, ICG, has been well-studied. It is safe at clinical doses, but higher doses may cause adverse effects [84]. Recently, a single dose short term toxicity study of Li-Cor's IRDye 800CW was completed in rats. Marshall *et al.* determined the carboxylate form of IRDye 800CW, the form used in conjugation, had no adverse effects when compared to ICG in either intravenous or intradermal administrations, and a dose of 20 mg/kg (10,000 times more than the projected clinical dose) did not cause observable adverse effects [85]. The data on the *in vivo* toxicity of other NIRF dyes, such as Cy5.5 and Cy7, have not been reported in literature. Because current studies using these fluorophores have mainly focused on their efficacies in NIRF imaging, little *in vivo* long-term toxicity has been reported. However, based on the literature, it is safe to say that the NIR fluorophores

used in animal studies do not appear to have acute toxicity. Long term *in vivo* toxicity studies would need to be performed in appropriate animal models before these fluorophores could be used in human clinical trials.

4.2. Non-specific uptake

Non-specific uptake by the reticuloendothelial system (RES) of the liver, spleen, lymph nodes, and bone marrow is a common phenomenon for systematically delivered reagents, including fluorescent probes. This non-specific uptake highly correlates to the dynamic size of the fluorescent probes and their conjugates; therefore, organic fluorophore conjugates have less non-specific uptake compared to QD conjugates [44,86]. A couple of studies have shown systematically delivered QDs were engulfed by macrophages after being retained in the sinusoidal vasculature of RES organs [86,87], greatly shortening their circulation half life. Alteration of the surface coating of QDs, such as introducing large molecular-weight PEG molecules, may reduce RES uptake and increase the circulating time of QDs in the blood stream, allowing more QDs to reach the target tumor [66]. In contrast to QDs, organic fluorophore conjugated antibodies have a much longer circulation half life and often reach the target tumor after one or two days of circulation [9,86].

5. Conclusion

NIRF imaging's ability to multiplex signals from different emission spectra, and potential for high spatial resolution and real-time display provide substantial advantages over conventional imaging techniques. These advantages explain the rapid development of NIRF imaging over the last twenty years and ensure this technology will continue to play an important role in research and clinical imaging.

6. Expert opinion

Among the NIRF imaging applications discussed in this review, SLN mapping and tumor margin definition do not require in depth imaging for clinical use. They pose few technical challenges and have already been used in human clinical trials. We predict that techniques using NIR fluorophores for tumor margin definition will enter the clinic in the near future. SLN mapping using NIR fluorophores may enter the clinic to sort the complicated lymphatic systems of visceral organs. In addition, one challenging area related to SLN mapping is to provide molecular signatures in lymph nodes. By administering conjugated fluorophores intravenously, one could identify metastases in the highly vascularized lymph nodes due to interactions between conjugated fluorophores and molecules on the surface of metastasized cells. The presence or absence of metastatic cells in the SLNs could be used to determine whether the removal of SLNs is necessary.

Conversely, studies on tumor targeting and characterization are exciting, but still in the early stages of development, due to several optical and biological obstacles. Some of these obstacles are improvable. For instance, there is often inadequate tumor signal over the background of surrounding tissues, due to nonspecific uptake and retention of the fluorophore conjugates. The development of "activatable probes" has proved successful in specific tumor targeting and reducing background. This issue could also be improved by developing fast clearing and less sticky fluorophore probes. Antibody-fluorophore conjugates have been reported to have low blood clearance and high non-specific uptake by the liver, consistent with the characteristics of antibodies themselves [8]. Small molecules or peptides are better choices to avoid this problem. Furthermore, advances in imaging equipment (such as cameras with enhanced sensitivity, and laser excitation sources for better penetration) and imaging methodology (such as fluorescence molecular tomography) may dramatically improve signal sensitivity. In addition to the issue of sensitivity, current

preclinical animal studies are mostly performed at the whole body level. Cellular and tissue localization of fluorophore conjugates have not been well described, and the pharmacodynamics and pharmacokinetics of fluorophore conjugates have not been thoroughly investigated. Moreover, the toxicity of most fluorophores is not reported in the same manner as would be reported for a new therapeutic drug. More research must be done to better understand the localization, pharmacokinetics, and pharacodynamics of NIR fluorophores, and careful toxicological studies must be carried out in appropriate animal models to establish their short and long term safety profiles.

Some of the obstacles that hinder NIRF's entrance into routine clinical practice are fundamental, such as the limited penetration depth due to signal attenuation of the fluorophores within tissue. The relatively large size and complexity of the human body may make non-invasive in-depth detection of NIRF signals in humans unlikely, at least in the near future. However, breakthroughs of NIRF imaging may follow the creation or discovery of novel fluorophores with low molecular weights and high extinction coefficients. The resulting high brightness of these fluorophores should partially overcome the obstacle of limited penetration, resulting in increased depth of imaging sensitivity.

We envision NIRF imaging readily used to diagnose and treat cancer in future clinical settings. To provide a hypothetical clinical scenario, we use a breast cancer example to show how corresponding treatment and monitoring could be improved. A diagnosis of breast cancer is frequently made with conventional imaging modalities, such as a mammogram or magnetic resonance imaging, followed by biopsy. During surgery, fluorophores can be applied to visually define tumor boundaries and map the SLNs. Detection of residual cells not visualized by conventional imaging techniques or pathologic examination of resected tissue, but seen by NIRF imaging might assist in treatment decisions. For example, if cells were still detectable in the breast, local treatment with radiotherapy would be advised while a "clean" NIRF imaging of the breast may allow the patient to avoid radiation therapy. Similarly, if NIRF imaging could detect distant micrometastatic cells, then systemic therapy (chemotherapy, hormonal therapy, targeted therapy, or a combination) could be used to eradicate these cells. In follow-up, the patient would be monitored for recurrence and/or metastasis by systematically delivered antibody-conjugated fluorophores. If early distant or local recurrences were detected, appropriate clinical action could be taken. In the case of distant recurrences, multiple fluorophores with distinct fluorescent spectra, each conjugated to antibodies against various molecular targets such as HER2, the type I IGF receptor, and EGFR, might be administrated systematically to the patient with the goal of prolonging survival. The fluorescence intensity would correlate with the level of each molecular target, and targeted therapies against overexpressed surface molecules would then be used to develop an individualized course of treatment. Overall, advancements in NIRF imaging could be used to lessen the burden of cancer. In this light, we foresee that NIRF imaging will become a vital part of clinical cancer imaging in the future.

References

1. Mankoff DA, Peterson LM, Tewson TJ, et al. [18F]fluoroestradiol radiation dosimetry in human PET studies. J Nucl Med. 2001; 42(4):679–684. [PubMed: 11337559]
2. Oude Munnink TH, Nagengast WB, Brouwers AH, et al. Molecular imaging of breast cancer. Breast. 2009; 18 (Suppl 3):S66–73. [PubMed: 19914546]
3. Perik PJ, Lub-De Hooge MN, Gietema JA, et al. Indium-111-labeled trastuzumab scintigraphy in patients with human epidermal growth factor receptor 2-positive metastatic breast cancer. J Clin Oncol. 2006; 24(15):2276–2282. [PubMed: 16710024]
4. Weissleder R, Ntziachristos V. Shedding light onto live molecular targets. Nat Med. 2003; 9(1): 123–128. [PubMed: 12514725]

5. Leblond F, Davis SC, Valdes PA, Pogue BW. Pre-clinical whole-body fluorescence imaging: Review of instruments, methods and applications. J Photochem Photobiol B. 2010; 98(1):77–94. [PubMed: 20031443]

6. Panchuk-Voloshina N, Haugland RP, Bishop-Stewart J, et al. Alexa dyes, a series of new fluorescent dyes that yield exceptionally bright, photostable conjugates. J Histochem Cytochem. 1999; 47(9):1179–1188. [PubMed: 10449539]

7. Berlier JE, Rothe A, Buller G, et al. Quantitative comparison of long-wavelength Alexa Fluor dyes to Cy dyes: fluorescence of the dyes and their bioconjugates. J Histochem Cytochem. 2003; 51(12): 1699–1712. [PubMed: 14623938]

8. Ogawa M, Regino CA, Choyke PL, Kobayashi H. In vivo target-specific activatable near-infrared optical labeling of humanized monoclonal antibodies. Mol Cancer Ther. 2009; 8(1):232–239. [PubMed: 19139133]

9. Ke S, Wen X, Gurfinkel M, et al. Near-infrared optical imaging of epidermal growth factor receptor in breast cancer xenografts. Cancer Res. 2003; 63(22):7870–7875. [PubMed: 14633715]

10. Achilefu S, Dorshow RB, Bugaj JE, Rajagopalan R. Novel receptor-targeted fluorescent contrast agents for in vivo tumor imaging. Invest Radiol. 2000; 35(8):479–485. [PubMed: 10946975]

11. Soukos NS, Hamblin MR, Keel S, et al. Epidermal growth factor receptor-targeted immunophotodiagnosis and photoimmunotherapy of oral precancer in vivo. Cancer Res. 2001; 61(11):4490–4496. [PubMed: 11389080]

12. Hines MA, Guyot-Sionnest P. Synthesis and characterization of strongly luminescing ZnS-Capped CdSe nanocrystals. J Phys Chem-Us. 1996; 100(2):468–471.

13. Dabbousi BO, RodriguezViejo J, Mikulec FV, et al. (CdSe)ZnS core-shell quantum dots: Synthesis and characterization of a size series of highly luminescent nanocrystallites. J Phys Chem B. 1997; 101(46):9463–9475.

14. Micic OI, Sprague JR, Curtis CJ, et al. Synthesis and Characterization of Inp, Gap, and Gainp2 Quantum Dots. J Phys Chem-Us. 1995; 99(19):7754–7759.

15*. Gao XH, Cui YY, Levenson RM, et al. In vivo cancer targeting and imaging with semiconductor quantum dots. Nature Biotechnology. 2004; 22:8–976. Reports that QDs can be conjugated with antibodies to target tumors *in vivo*.

16. Alivisatos AP. Semiconductor clusters, nanocrystals, and quantum dots. Science. 1996; 271(5251): 933–937.

17. Kim S, Bawendi MG. Oligomeric Ligands for luminescent and stable nanocrystal quantum dots. J Am Chem Soc. 2003; 125(48):14652–14653. [PubMed: 14640609]

18*. Kim S, Lim YT, Soltesz EG, et al. Near-infrared fluorescent type II quantum dots for sentinel lymph node mapping. Nature Biotechnology. 2004; 22(1):93–97. First report for QDs application in SLN mapping.

19. Hama Y, Koyama Y, Urano Y, et al. Simultaneous two-color spectral fluorescence lymphangiography with near infrared quantum dots to map two lymphatic flows from the breast and the upper extremity. Breast Cancer Res Treat. 2007; 103(1):23–28. [PubMed: 17028977]

20. Zhang H, Sachdev D, Wang C, et al. Detection and downregulation of type I IGF receptor expression by antibody-conjugated quantum dots in breast cancer cells. Breast Cancer Res Treat. 2009; 114(2):277–285. [PubMed: 18418709]

21**. Kobayashi H, Hama Y, Koyama Y, et al. Simultaneous multicolor imaging of five different lymphatic basins using quantum dots. Nano Lett. 2007; 7(6):1711–1716. Simultaneous mapping of the complicated lymphatic systems using QDs. [PubMed: 17530812]

22. He X, Chen J, Wang K, et al. Preparation of luminescent Cy5 doped core-shell SFNPs and its application as a near-infrared fluorescent marker. Talanta. 2007; 72(4):1519–1526. [PubMed: 19071792]

23. Wang L, Yang C, Tan W. Dual-luminophore-doped silica nanoparticles for multiplexed signaling. Nano Lett. 2005; 5(1):37–43. [PubMed: 15792409]

24. Jiang S, Gnanasammandhan MK, Zhang Y. Optical imaging-guided cancer therapy with fluorescent nanoparticles. J R Soc Interface. 2010; 7(42):3–18. [PubMed: 19759055]

25. Newman EA, Newman LA. Lymphatic mapping techniques and sentinel lymph node biopsy in breast cancer. Surg Clin N Am. 2007; 87(2):353–+. [PubMed: 17498531]

26. Knapp DW, Adams LG, Degrand AM, et al. Sentinel Lymph Node Mapping of Invasive Urinary Bladder Cancer in Animal Models Using Invisible Light. Eur Urol. 2007
27. Soltesz EG, Kim S, Kim SW, et al. Sentinel lymph node mapping of the gastrointestinal tract by using invisible light. Ann Surg Oncol. 2006; 13(3):386–396. [PubMed: 16485157]
28. Soltesz EG, Kim S, Laurence RG, et al. Intraoperative sentinel lymph node mapping of the lung using near-infrared fluorescent quantum dots. Ann Thorac Surg. 2005; 79(1):269–277. [PubMed: 15620956]
29. Parungo CP, Ohnishi S, Kim SW, et al. Intraoperative identification of esophageal sentinel lymph nodes with near-infrared fluorescence imaging. J Thorac Cardiov Sur. 2005; 129(4):844–850.
30. Grayburn PA. Current and future contrast agents. Echocardiography. 2002; 19(3):259–265. [PubMed: 12022935]
31. Stanga PE, Lim JI, Hamilton P. Indocyanine green angiography in chorioretinal diseases: indications and interpretation: an evidence-based update. Ophthalmology. 2003; 110(1):15–21. quiz 22-13. [PubMed: 12511340]
32. Demers ML, Ellis LM, Roh MS. Surgical management of hepatoma. Cancer Treat Res. 1994; 69:277–290. [PubMed: 8031657]
33. Kitai T, Inomoto T, Miwa M, Shikayama T. Fluorescence navigation with indocyanine green for detecting sentinel lymph nodes in breast cancer. Breast Cancer. 2005; 12(3):211–215. [PubMed: 16110291]
34. Tagaya N, Yamazaki R, Nakagawa A, et al. Intraoperative identification of sentinel lymph nodes by near-infrared fluorescence imaging in patients with breast cancer. Am J Surg. 2008; 195(6): 850–853. [PubMed: 18353274]
35. Fujiwara M, Mizukami T, Suzuki A, Fukamizu H. Sentinel lymph node detection in skin cancer patients using real-time fluorescence navigation with indocyanine green: preliminary experience. J Plast Reconstr Aesthet Surg. 2009; 62(10):e373–378. [PubMed: 18556255]
36. Sevick-Muraca EM, Sharma R, Rasmussen JC, et al. Imaging of lymph flow in breast cancer patients after microdose administration of a near-infrared fluorophore: feasibility study. Radiology. 2008; 246(3):734–741. [PubMed: 18223125]
37. Aikou T, Kitagawa Y, Kitajima M, et al. Sentinel lymph node mapping with GI cancer. Cancer Metast Rev. 2006; 25(2):269–277.
38. Hama Y, Koyama Y, Urano Y, et al. Two-color lymphatic mapping using Ig-conjugated near infrared optical probes. J Invest Dermatol. 2007; 127(10):2351–2356. [PubMed: 17522707]
39. Kobayashi H, Koyama Y, Barrett T, et al. Multimodal nanoprobes for radionuclide and five-color near-infrared optical lymphatic imaging. ACS Nano. 2007; 1(4):258–264. [PubMed: 19079788]
40. Mukherjee P, Tinder TL, Basu GD, et al. Therapeutic efficacy of MUC1-specific cytotoxic T lymphocytes and CD137 co-stimulation in a spontaneous breast cancer model. Breast Dis. 2004; 20:53–63. [PubMed: 15687707]
41. Schulke N, Varlamova OA, Donovan GP, et al. The homodimer of prostate-specific membrane antigen is a functional target for cancer therapy. Proc Natl Acad Sci U S A. 2003; 100(22):12590–12595. [PubMed: 14583590]
42. Weitman SD, Lark RH, Coney LR, et al. Distribution of the folate receptor GP38 in normal and malignant cell lines and tissues. Cancer Res. 1992; 52(12):3396–3401. [PubMed: 1596899]
43. Gatter KC, Brown G, Trowbridge IS, et al. Transferrin receptors in human tissues: their distribution and possible clinical relevance. J Clin Pathol. 1983; 36(5):539–545. [PubMed: 6302135]
44. Ma L, Yu P, Veerendra B, et al. In vitro and in vivo evaluation of Alexa Fluor 680-bombesin[7–14]NH2 peptide conjugate, a high-affinity fluorescent probe with high selectivity for the gastrin-releasing peptide receptor. Mol Imaging. 2007; 6(3):171–180. [PubMed: 17532883]
45. Miki K, Oride K, Inoue S, et al. Ring-opening metathesis polymerization-based synthesis of polymeric nanoparticles for enhanced tumor imaging in vivo: Synergistic effect of folate-receptor targeting and PEGylation. Biomaterials. 2010; 31(5):934–942. [PubMed: 19853909]
46. Humblet V, Lapidus R, Williams LR, et al. High-affinity near-infrared fluorescent small-molecule contrast agents for in vivo imaging of prostate-specific membrane antigen. Mol Imaging. 2005; 4(4):448–462. [PubMed: 16285907]

47. Lee SB, Hassan M, Fisher R, et al. Affibody molecules for in vivo characterization of HER2-positive tumors by near-infrared imaging. Clin Cancer Res. 2008; 14(12):3840–3849. [PubMed: 18559604]

48. Sampath L, Kwon S, Ke S, et al. Dual-labeled trastuzumab-based imaging agent for the detection of human epidermal growth factor receptor 2 overexpression in breast cancer. J Nucl Med. 2007; 48(9):1501–1510. [PubMed: 17785729]

49**. Koyama Y, Barrett T, Hama Y, et al. In vivo molecular imaging to diagnose and subtype tumors through receptor-targeted optically labeled monoclonal antibodies. Neoplasia. 2007; 9(12):1021–1029. A pioneer study of activatale fluorescent probes *in vivo*. [PubMed: 18084609]

50. Barrett T, Koyama Y, Hama Y, et al. In vivo diagnosis of epidermal growth factor receptor expression using molecular imaging with a cocktail of optically labeled monoclonal antibodies. Clin Cancer Res. 2007; 13(22 Pt 1):6639–6648. [PubMed: 17982120]

51. Weissleder R, Tung CH, Mahmood U, Bogdanov A Jr. In vivo imaging of tumors with protease-activated near-infrared fluorescent probes. Nat Biotechnol. 1999; 17(4):375–378. [PubMed: 10207887]

52. Mahmood U, Weissleder R. Near-infrared optical imaging of proteases in cancer. Mol Cancer Ther. 2003; 2(5):489–496. [PubMed: 12748311]

53. Bremer C, Bredow S, Mahmood U, et al. Optical imaging of matrix metalloproteinase–2 activity in tumors: feasibility study in a mouse model. Radiology. 2001; 221(2):523–529. [PubMed: 11687699]

54. Jiang T, Olson ES, Nguyen QT, et al. Tumor imaging by means of proteolytic activation of cell-penetrating peptides. Proc Natl Acad Sci U S A. 2004; 101(51):17867–17872. [PubMed: 15601762]

55. Aguilera TA, Olson ES, Timmers MM, et al. Systemic in vivo distribution of activatable cell penetrating peptides is superior to that of cell penetrating peptides. Integr Biol (Camb). 2009; 1(5–6):371–381. [PubMed: 20023744]

56*. Olson ES, Jiang T, Aguilera TA, et al. Activatable cell penetrating peptides linked to nanoparticles as dual probes for in vivo fluorescence and MR imaging of proteases. Proc Natl Acad Sci U S A. 2010; 107(9):4311–4316. Reports another type of activatable fluorescent probes *in vivo*. [PubMed: 20160077]

57. Olson ES, Aguilera TA, Jiang T, et al. In vivo characterization of activatable cell penetrating peptides for targeting protease activity in cancer. Integr Biol (Camb). 2009; 1(5–6):382–393. [PubMed: 20023745]

58. Alencar H, Funovics MA, Figueiredo J, et al. Colonic adenocarcinomas: near-infrared microcatheter imaging of smart probes for early detection-–study in mice. Radiology. 2007; 244(1):232–238. [PubMed: 17507718]

59. Sheth RA, Upadhyay R, Stangenberg L, et al. Improved detection of ovarian cancer metastases by intraoperative quantitative fluorescence protease imaging in a pre-clinical model. Gynecol Oncol. 2009; 112(3):616–622. [PubMed: 19135233]

60. Figueiredo JL, Alencar H, Weissleder R, Mahmood U. Near infrared thoracoscopy of tumoral protease activity for improved detection of peripheral lung cancer. Int J Cancer. 2006; 118(11): 2672–2677. [PubMed: 16380983]

61. Parks WC, Wilson CL, Lopez-Boado YS. Matrix metalloproteinases as modulators of inflammation and innate immunity. Nat Rev Immunol. 2004; 4(8):617–629. [PubMed: 15286728]

62*. Ogawa M, Kosaka N, Longmire MR, et al. Fluorophore-quencher based activatable targeted optical probes for detecting in vivo cancer metastases. Mol Pharm. 2009; 6(2):386–395. Reports another type of activatable fluorescent probes in vivo. [PubMed: 19718793]

63. Ogawa M, Kosaka N, Choyke PL, Kobayashi H. In vivo molecular imaging of cancer with a quenching near-infrared fluorescent probe using conjugates of monoclonal antibodies and indocyanine green. Cancer Res. 2009; 69(4):1268–1272. [PubMed: 19176373]

64. Ogawa M, Kosaka N, Choyke PL, Kobayashi H. Tumor-specific detection of an optically targeted antibody combined with a quencher-conjugated neutravidin "quencher-chaser": a dual "quench and chase" strategy to improve target to nontarget ratios for molecular imaging of cancer. Bioconjug Chem. 2009; 20(1):147–154. [PubMed: 19072537]

65. Diagaradjane P, Orenstein-Cardona JM, NEC-C, et al. Imaging epidermal growth factor receptor expression in vivo: pharmacokinetic and biodistribution characterization of a bioconjugated quantum dot nanoprobe. Clin Cancer Res. 2008; 14(3):731–741. [PubMed: 18245533]
66. Akerman ME, Chan WCW, Laakkonen P, et al. Nanocrystal targeting in vivo. P Natl Acad Sci USA. 2002; 99(20):12617–12621.
67. Laakkonen P, Akerman ME, Biliran H, et al. Antitumor activity of a homing peptide that targets tumor lymphatics and tumor cells. P Natl Acad Sci USA. 2004; 101(25):9381–9386.
68. Yong KT, Hu R, Roy I, et al. Tumor targeting and imaging in live animals with functionalized semiconductor quantum rods. ACS Appl Mater Interfaces. 2009; 1(3):710–719. [PubMed: 20160901]
69. Tada H, Higuchi H, Wanatabe TM, Ohuchi N. In vivo real-time tracking of single quantum dots conjugated with monoclonal anti-HER2 antibody in tumors of mice. Cancer Res. 2007; 67(3): 1138–1144. [PubMed: 17283148]
70. Yang L, Mao H, Wang YA, et al. Single chain epidermal growth factor receptor antibody conjugated nanoparticles for in vivo tumor targeting and imaging. Small. 2009; 5(2):235–243. [PubMed: 19089838]
71. Li SD, Huang L. Pharmacokinetics and Biodistribution of Nanoparticles. Mol Pharm. 2008
72. Haglund MM, Berger MS, Hochman DW. Enhanced optical imaging of human gliomas and tumor margins. Neurosurgery. 1996; 38(2):308–317. [PubMed: 8869058]
73. Gotoh K, Yamada T, Ishikawa O, et al. A novel image-guided surgery of hepatocellular carcinoma by indocyanine green fluorescence imaging navigation. J Surg Oncol. 2009; 100(1):75–79. [PubMed: 19301311]
74. Nguyen QT, Olson ES, Aguilera TA, et al. Surgery with molecular fluorescence imaging using activatable cell-penetrating peptides decreases residual cancer and improves survival. Proc Natl Acad Sci U S A. 2010; 107(9):4317–4322. [PubMed: 20160097]
75*. Choi HS, Liu W, Misra P, et al. Renal clearance of quantum dots. Nat Biotechnol. 2007; 25(10): 1165–1170. A pioneer study on the renal clearance of QDs. [PubMed: 17891134]
76. Derfus AMC, WCW, Bhatia SN. Probing the cytotoxicity of semiconductor quantum dots. Nano letters. 2004; 4(1):11–18.
77. Chen LD, Liu J, Yu XF, et al. The biocompatibility of quantum dot probes used for the targeted imaging of hepatocellular carcinoma metastasis. Biomaterials. 2008; 29(31):4170–4176. [PubMed: 18691751]
78. Ballou B, Ernst LA, Andreko S, et al. Sentinel lymph node imaging using quantum dots in mouse tumor models. Bioconjug Chem. 2007; 18(2):389–396. [PubMed: 17263568]
79. Mangolini L, Jurbergs D, Rogojina E, Kortshagen U. Plasma synthesis and liquid-phase surface passivation of brightly luminescent Si nanocrystals. J Lumin. 2006; 121(2):327–334.
80. Mangolini L, Thimsen E, Kortshagen U. High-yield plasma synthesis of luminescent silicon nanocrystals. Nano Letters. 2005; 5(4):655–659. [PubMed: 15826104]
81. Cheng KY, Anthony R, Kortshagen UR, Holmes RJ. Hybrid silicon nanocrystal-organic light–emitting devices for infrared electroluminescence. Nano Lett. 2010; 10(4):1154–1157. [PubMed: 20337448]
82. O'Farrell N, Houlton A, Horrocks BR. Silicon nanoparticles: applications in cell biology and medicine. Int J Nanomedicine. 2006; 1(4):451–472. [PubMed: 17722279]
83. Alford R, Simpson HM, Duberman J, et al. Toxicity of organic fluorophores used in molecular imaging: literature review. Mol Imaging. 2009; 8(6):341–354. [PubMed: 20003892]
84. Hope-Ross M, Yannuzzi LA, Gragoudas ES, et al. Adverse reactions due to indocyanine green. Ophthalmology. 1994; 101(3):529–533. [PubMed: 8127574]
85. Marshall MV, Draney D, Sevick-Muraca EM, Olive DM. Single-dose intravenous toxicity study of IRDye 800CW in Sprague-Dawley rats. Mol Imaging Biol. 2010; 12(6):583–594. [PubMed: 20376568]
86. Zhang H, Zeng X, Li Q, et al. Fluorescent tumour imaging of type I IGF receptor in vivo: comparison of antibody–conjugated quantum dots and small-molecule fluorophore. Br J Cancer. 2009; 101(1):71–79. [PubMed: 19491901]

87. Jackson H, Muhammad O, Daneshvar H, et al. Quantum dots are phagocytized by macrophages and colocalize with experimental gliomas. Neurosurgery. 2007; 60(3):524–529. discussion 529–530. [PubMed: 17327798]

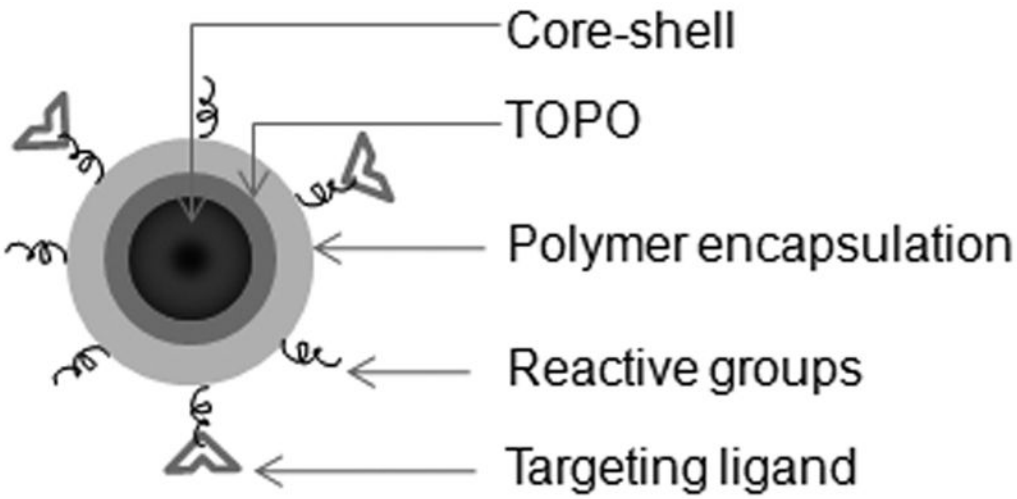

Fig. 1.
Schematic of quantum dots (QDs).

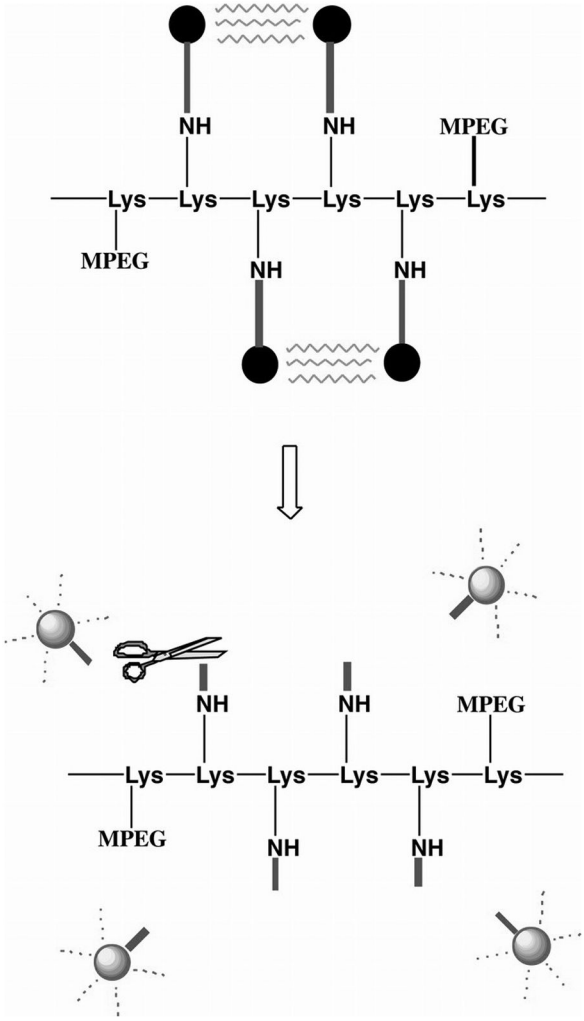

Fig. 2.

Schematic shows design of the MMP-2-sensitive fluorescent probe for in vivo NIRF imaging. Fluorophores with excitation and emission wavelengths in the NIR spectrum were covalently coupled to a poly-l-lysine backbone (—Lys-Lys-Lys…—) sterically protected by methoxy polyethylene glycol (MPEG) side chains by means of a synthetic MMP-2 peptide substrate. Top: Owing to the proximity of the fluorophores, fluorescence resonance energy transfer occurs so that almost no fluorescent signal can be detected in the nonactivated state. Bottom: After MMP-2 cleavage of the peptide spacer, fluorophores are released from the carrier and become brightly fluorescent. Figure is reproduced and modified with permission from *Radiology* [53]. “Copyright (2001) The Radiological Society of North America (RSNA)”.

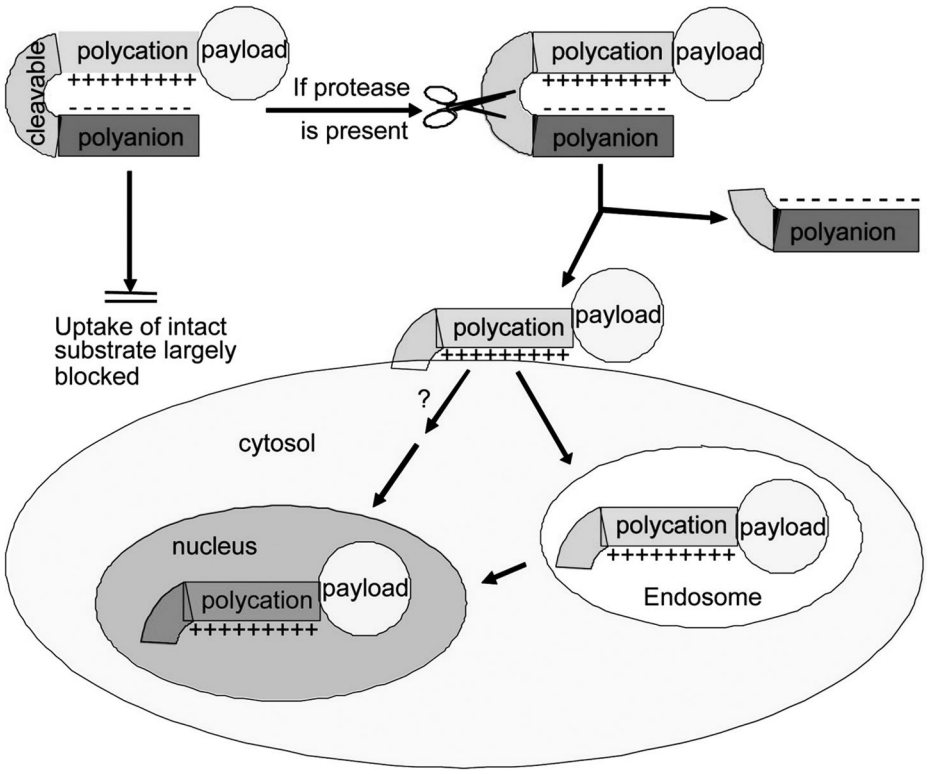

Fig. 3.

Schematic diagram of activatable CPPs. Cellular uptake induced by a cationic peptide is blocked by a short stretch of acidic residues attached by a cleavable linker. Once the linker is cleaved, the acidic inhibitory domain drifts away, and the cationic CPP is free to carry its cargo into cells. Figure is reproduced and modified with permission from *Proc Natl Acad Sci U S A* [54]. "Copyright (2004) National Academy of Sciences, U.S.A."